

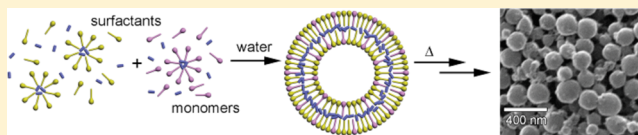
Directed Assembly of Vesicle-Templated Polymer Nanocapsules under Near-Physiological Conditions

Mariya D. Kim, Sergey A. Dergunov, and Eugene Pinkhassik*

Department of Chemistry, University of Connecticut, 55 North Eagleville Road, Storrs, Connecticut 06269-3060, United States

 Supporting Information

ABSTRACT: This work addresses the challenge of creating hollow polymer capsules with wall thickness in the single-nanometer range under mild conditions. We present a simple and scalable method for the synthesis of hollow polymer nanocapsules in the bilayers of spontaneously assembled surfactant vesicles. Polymerization is initiated thermally with the help of a peroxide initiator and an amine activator codissolved with monomers and cross-linkers in the hydrophobic interior of the surfactant bilayer. To avoid premature polymerization, the initiator and the activator were added separately to the mixtures of cetyltrimethylammonium tosylate (CTAT) and sodium dodecylbenzenesulfonate (SDBS) containing monomers and cross-linkers. Upon hydration and mixing of the aqueous solutions, equilibrium monomer-loaded vesicles formed spontaneously after a brief incubation. The removal of oxygen and further incubation at slightly elevated temperatures ($35\text{--}40\text{ }^{\circ}\text{C}$) for 1 to 2 h has led to the formation of hollow polymer nanocapsules. Structural and permeability characterization supported the high yield of nanocapsules with no pinhole defects.



1. INTRODUCTION

Here we describe the successful synthesis of polymer nanocapsules accomplished under mild conditions by directed assembly in the interior of bilayers of self-assembled vesicles. Previously, we and others synthesized a broad range of bilayer-templates structures, including nanocapsules, nanorattles, nanodisks, and nanorods.^{1–10} Nanocapsule-based structures show promise as nanosensors, nanoreactors, and other functional nanodevices as well as vehicles for drug delivery and the investigation of compartmentalization and interactions between biomolecules.^{11–13} Current methods for the synthesis of nanocapsules require irradiation with UV light or polymerization at fairly high temperatures exceeding $60\text{--}70\text{ }^{\circ}\text{C}$. These conditions are detrimental to most biological molecules, e.g., proteins, and many light-sensitive molecules that could be used as imaging contrasts or chemosensors, whereas these molecules are especially attractive for practical applications. The encapsulation of molecules sensitive to light and/or temperature requires new synthesis methods. In particular, the synthesis of nanocapsules under conditions close to physiological is likely to prove extremely useful.

The directed covalent assembly of organic nanostructures using temporary scaffolds can be done via the creation of self-assembled amphiphilic scaffolds loaded with hydrophobic monomers followed by polymerization and scaffold removal to yield stable cross-linked structures. Lipids and catanionic surfactants (mixture of cationic and anionic surfactants) have been used successfully as self-assembled scaffolds.^{4,8,14–16} Different styrene and acrylic monomers and cross-linkers were polymerized in the hydrophobic interior of self-assembled scaffolds, primarily bilayers, to produce self-standing structures, including nanocapsules, nanodisks, nanorattles, and nano-

rods.^{1–10} Codissolving pore-forming templates in the hydrophobic interior of bilayers of vesicles has led to the formation of pores with a controlled size and chemical environment.^{17,18}

Kaler et al. showed the synthesis of polymer particles based on styrene monomers in bilayers of surfactant vesicles at temperatures of $60\text{--}65\text{ }^{\circ}\text{C}$, where hydrophobic monomers were added to the aqueous suspension of vesicles after 1 day of equilibration and initiator was injected into the reaction mixture.^{16,19} Meier and others used vesicles formed by lipids or catanionic surfactants as templates for the synthesis of polymer nanocapsules.^{15,16,20–22} More recently, Forcada reported the synthesis and detailed characterization of nanocapsules produced by vesicle templating.²³ In earlier studies, monomers were typically added to the aqueous suspension of self-assembled vesicles and allowed to diffuse into the hydrophobic interior of bilayers (diffusion loading).^{24,25} Recently, we reported that bilayers could be loaded with monomers during the vesicle-formation stage (concurrent loading).^{2,26} In fact, in certain cases, the presence of monomers favored the spontaneous assembly of surfactants into vesicles.²⁷

Nanostructures produced by the directed assembly approach show significant promise in different applications. Vesicle-templated nanocapsules can be used as a platform for the creation of nanoreactors, nanosensors, and vehicles for the uptake and release of drugs or imaging contrasts. Encapsulation improved the stability of photosensitive molecules.²⁸ In related studies, Nolte and van Hest demonstrated the feasibility of assembling nanobioreactors using enzymes entrapped in

Received: November 26, 2014

Revised: January 8, 2015

Published: January 8, 2015

polymersomes.^{29–34} Vesicle-templated nanocapsules offer many advantages compared to other hollow polymer structures, including excellent control of permeability, ultrafast diffusion, and long-term stability.^{2,3,17,18} Precise permeability control and ultrafast diffusion are enabled by robust capsule shells with single-nanometer thickness. In contrast, hollow polymer nano- and microcapsules prepared by other methods, including emulsion-based processes or templating with a sacrificial core, have shells thicknesses typically ranging from tens to hundreds of nanometers.^{35–39} Expanding the vesicle-templated nanocapsule platform to the application involving enzymes or other biomolecules and different indicator dyes would undoubtedly advance the field of functional nanodevices.

Current methods for the synthesis of vesicle-templated nanocapsules involve either prolonged UV irradiation or exposure to high temperature. These conditions are not compatible with a large number of molecules, including biomolecules, e.g., enzymes, and UV-degradable dyes. In addition, the creation of nanocapsules containing indicator dyes presents difficulties for scaling up the synthesis when UV-initiated polymerization is used because the dyes absorb UV light and decrease the effective penetration depth of the radiation. This work focuses on establishing robust methods for the synthesis of polymer shells within a hydrophobic interior of a vesicular bilayer under mild conditions resembling physiological conditions. Kinetic experiments provided further insights into the formation of a polymer shell, and a detailed characterization of nanocapsules showed the successful creation of nanometer-thick shells with no pinhole defects.

2. EXPERIMENTAL SECTION

2.1. Monomers. Butyl methacrylate (BMA), *t*-butyl methacrylate (*t*-BMA), ethylene glycol dimethacrylate (EGDMA), 4-*tert*-butylstyrene (TBS), and divinylbenzene (DVB) were received from Sigma-Aldrich. They were purified by passing through aluminum oxide shortly before synthesis. Sodium dodecylbenzenesulfonate (SDBS, an anionic surfactant), cetyltrimethylammonium *p*-toluenesulfonate (CTAT, a cationic surfactant), lauroyl peroxide (LP, an initiator), and 4,4'-methylenebis(*N,N*-dimethylaniline) (MDA, an activator) were used as received (Sigma-Aldrich). Procion turquoise MX-G (PT) (received from DyStar) and Procion red MX 5B (PR) (received from Sigma-Aldrich) dyes were deactivated in a 0.1 wt % Na₂CO₃ aqueous solution overnight at room temperature to substitute active –Cl groups by –OH groups;⁴⁰ 4-(phenylazo)benzoic acid (PBA) (Sigma-Aldrich) was used as received.

2.2. Concurrent Loading of Monomers into Surfactant Vesicles. To prepare stock solutions, SDBS (100 mg) was mixed with acrylic monomers *t*-BMA (32 μL, 0.193 mmol), BMA (32 μL, 0.199 mmol), and EGDMA (32 μL, 0.166 mmol) or styrene monomers TBS (52.06 μL) and DVB (40.45 μL) and initiator LP. The amounts of initiator were varied so as to achieve concentrations between 1×10^{-4} and 4×10^{-4} M with the ratio of monomers to initiator between 570:1 and 140:1 in the final aqueous solutions after mixing SDBS and CTAT stock solutions. CTAT (100 mg) was mixed with *t*-BMA (32 μL, 0.193 mmol), BMA (32 μL, 0.199 mmol), and EGDMA (32 μL, 0.166 mmol) or styrene monomers TBS (52.06 μL) and DVB (40.45 μL) and activator MDA. The amounts of MDA were varied to achieve concentrations between 0.5×10^{-4} and 4×10^{-4} M with the ratio of monomers to activator between 1140:1 and 140:1 in the final aqueous solutions after mixing SDBS and CTAT stock solutions. Each mixture was hydrated in 10 mL of deionized water or dye solutions. The CTAT stock solution was equilibrated at 40 °C for 30 min. Samples were prepared by mixing the stock solutions in the proper volume ratios after brief vortex mixing, and the solutions were not subjected to any type of mechanical agitation and were additionally equilibrated at room temperature for 1 h or were extruded five times at

25 °C through a track-etched polyester Nucleopore membrane (Sterlytech) with a 0.2 μm pore size using a Lipex stainless steel extruder (Northern Lipids).

2.3. Synthesis of Nanocapsules. The suspension of monomer-loaded vesicles prepared as described above was purged with nitrogen and set to incubate in the thermostated bath at the desired temperature. Following polymerization, a solution of NaCl (3 drops or approx. 0.02 mL of a 3 M aqueous solution) in methanol (10 mL) was added to the reaction mixture to precipitate the nanocapsules. The nanocapsules were separated from the reaction mixture and purified by repeated centrifugation and resuspension steps using methanol (3 drops or approx. 0.02 mL of a 3 M aqueous NaCl solution was added to aid precipitation), then methanol–water mixtures (methanol:water ratio changing from approx. 5:1 to 1:5), and finally water as washing solutions. A suspension of nano capsules was centrifuged after each washing at approx. 2000g for 5 min.

2.4. Dynamic Light Scattering (DLS). Hydrodynamic diameter and polydispersity index (PDI) measurements were performed on a Malvern Nano-ZS Zetasizer (Malvern Instruments Ltd., Worcestershire, U.K.). The helium–neon laser, 4 mW, operated at 633 nm with a scattering angle fixed at 173° and a temperature of 25 °C. Samples (80 μL each) were placed in disposable cuvettes without dilution (70 μL, 8.5 mm center height UV-cuvette micro). Each data point was an average of 10 scans. Data were processed using non-negative least-squares (NNLS) analysis.

2.5. Electron Microscopy Images. SEM and TEM images were obtained with a FEI Inspect F50 STEM scanning electron microscope (Hillsboro, OR) at a working voltage of 30 kV. To prepare the sample for TEM analysis, a drop of sample was carefully placed on a 200-mesh carbon grid, and excess sample was wiped away with filter paper. Then a drop of 2% uranyl acetate (same pH as the sample) was added to the grid to negatively stain the sample. After 2 min, the excess liquid was wiped off. To prepare the sample for SEM analysis, a drop of an aqueous sample was placed on an SEM pin stub specimen mount covered with double-coated carbon conductive tabs and dried under vacuum. The studied samples were coated with a 5 nm gold layer using an EMS 590 X sputterer (Hatfield, PA).

2.6. NMR Measurements. A Bruker 400 MHz broadband NMR spectrometer was used to collect data for all kinetics experiments using tetramethylsilane as an internal standard ($\delta = 0$ ppm). For kinetic experiments, different aliquots of monomers and initiator were mixed with 50 mg of SDBS. Similarly, CTAT (50 mg) was mixed with different aliquots of monomers with activator. Each mixture was hydrated in 5 mL of D₂O. The CTAT stock solution was equilibrated at 40 °C for 30 min. Samples for NMR measurements were prepared by mixing the stock solutions in appropriate volume ratios followed by brief vortex mixing. The solutions were not subjected to any type of further mechanical agitation and were additionally equilibrated at room temperature for 1 h. The suspension of monomer-loaded vesicles was transferred to the NMR tube, purged with nitrogen, and set to equilibrate in the NMR spectrometer at the desired temperature. Measurements were taken at regular time intervals to determine the conversion of monomers. Signals at 5.7 and 5.9 ppm (hydrogens attached to the carbon–carbon double bond) were used to monitor the polymerization. Characteristic peaks from surfactant molecules (7–7.6 ppm) were used as an internal reference because they did not change during the polymerization process.

2.7. Dye Retention Experiment. A previously described colored size-probe retention assay was used to demonstrate the successful formation of nanocapsules formed by the new thermal initiation method.¹⁷ Molecules with different colors and sizes were encapsulated in surfactant vesicles, polymerization was carried out, and nanocapsules were separated from released size probes on a size-exclusion column and/or by the precipitation of nanocapsules in methanol and purification by repeated centrifugation and resuspension steps using methanol (3 drops of NaCl (3 M) was added to aid precipitation), then methanol–water mixtures (methanol:water ratio changing from approx 5:1 to 1:5), and water as washing solutions. The following size probes were used to gauge the pore size: yellow, 0.6 nm probe (4-

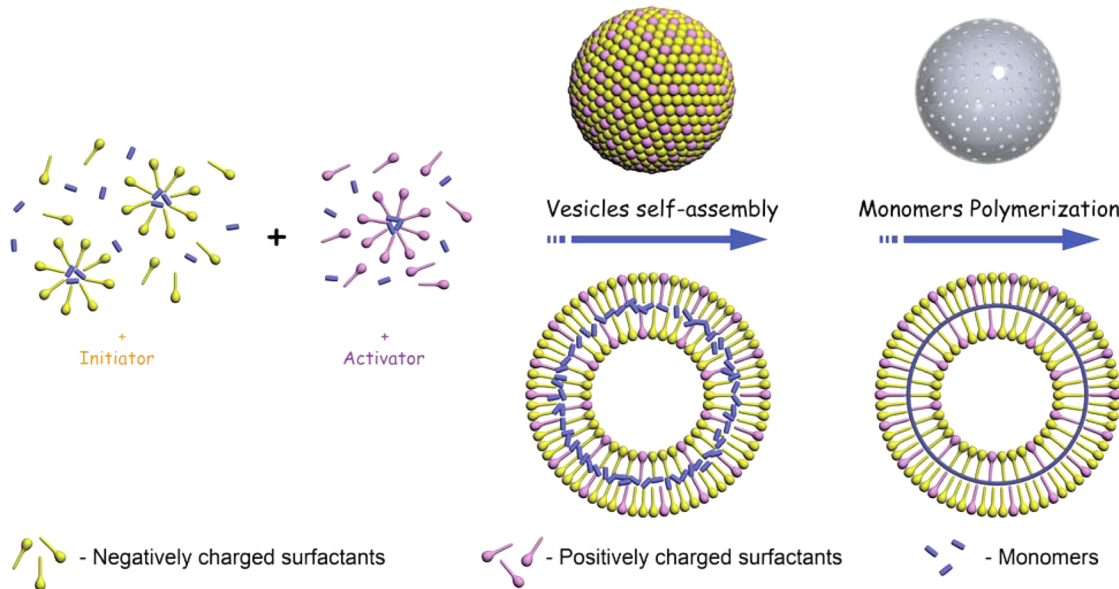
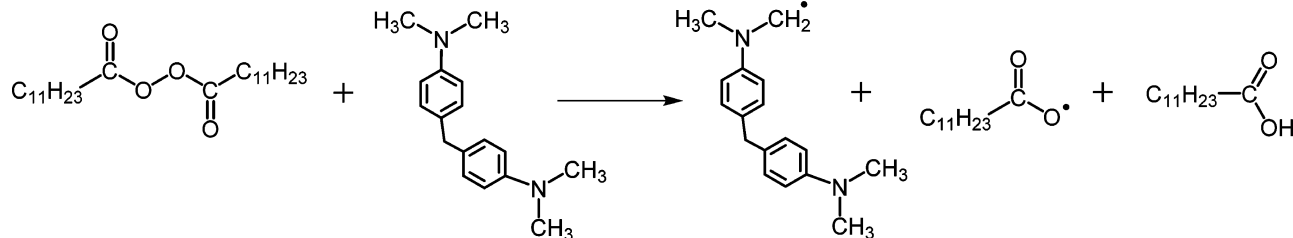


Figure 1. Spontaneous formation of surfactant vesicles in the presence of hydrophobic monomers and the polymerization of monomers inside the bilayer.

Scheme 1. Formation of Radicals from Lauroyl Peroxide (Initiator) and 4,4'-Methylenebis(*N,N*-dimethylaniline) (Activator)



(phenylazo)benzoic acid, PBA); red, 1.1 nm probe (Procion red, PR); and blue, 1.3 nm probe (Procion turquoise MX-G, PT).^{17,24}

3. RESULTS AND DISCUSSION

The goal of this work is to accomplish the polymerization of monomers and cross-linkers in the interior of a bilayer formed by surfactants or lipids (Figure 1) under mild conditions close to the physiological range, i.e., neutral pH and temperature between 35 and 40 °C. In this work, we focus on the vesicles formed by catanionic surfactants. The monomers and cross-linkers are placed into the bilayer interior during the self-assembly of vesicles (concurrent loading). We and others have shown previously that monomers can also be loaded into catanionic vesicles after vesicle assembly (diffusion loading) and that liposomes can be loaded with monomers using either concurrent loading or diffusion loading methods.^{2,4,24–27} We believe that the methodology established in this work will be readily transferable to any vesicular structure containing monomers in the hydrophobic interior.

Our approach is based on the thermal initiation of polymerization assisted by the combined use of initiator and activator molecules. Previous studies showed that the bulk polymerization of neat acrylic and styrene-based monomers could occur at fairly low temperatures when tertiary amines were present in the mixture with peroxides.^{41–47} To perform the polymerization in the hydrophobic interior of bilayers, the initiator and activator molecules should be colocated in the bilayer interior with monomers and cross-linkers. We chose

lauroyl peroxide as a highly hydrophobic molecule that would be dissolved in the interior of the surfactant bilayer. We further selected 4,4'-methylenebis(*N,N*-dimethylaniline) as an activator because of its combination of the proper hydrophobic/hydrophilic balance and the temperature of initiation. Wilson et al.⁴⁸ compared different activators and showed that 4,4'-methylenebis(*N,N*-dimethylaniline) with two tertiary amine groups reacts at lower temperatures than does 4-*N,N*-trimethylaniline or *N,N*-dimethylaniline, other common commercially available activators. After oxygen removal, the initiator/activator pair generates free radicals as shown in Scheme 1. We selected catanionic vesicles prepared from SDBS and CTAT in an 80:20 weight ratio. The monomers and cross-linkers were placed into the interior of bilayers via concurrent loading, i.e., vesicles were formed in the presence of monomers as described previously.^{26,27} Before the detailed investigation of the polymerization, we examined the stability of surfactant/monomers vesicles at various temperatures. Dynamic light scattering (DLS) analysis revealed structures with an average diameter of 220 ± 10 nm and a polydispersity index (PDI) of 0.2–0.4 (Figure S1). PDI in the observed range is typically indicative of a narrow size distribution.^{26,49} No evidence of large aggregates was found for acrylic monomers at various temperatures (Figure S1A), but DLS of catanionic vesicles loaded with styrene monomers showed a small number of aggregates under the same conditions (Figure S1B). These data are consistent with our previous report showing a loaded vesicle phase in the greater concentration/surfactant ratio ranges for

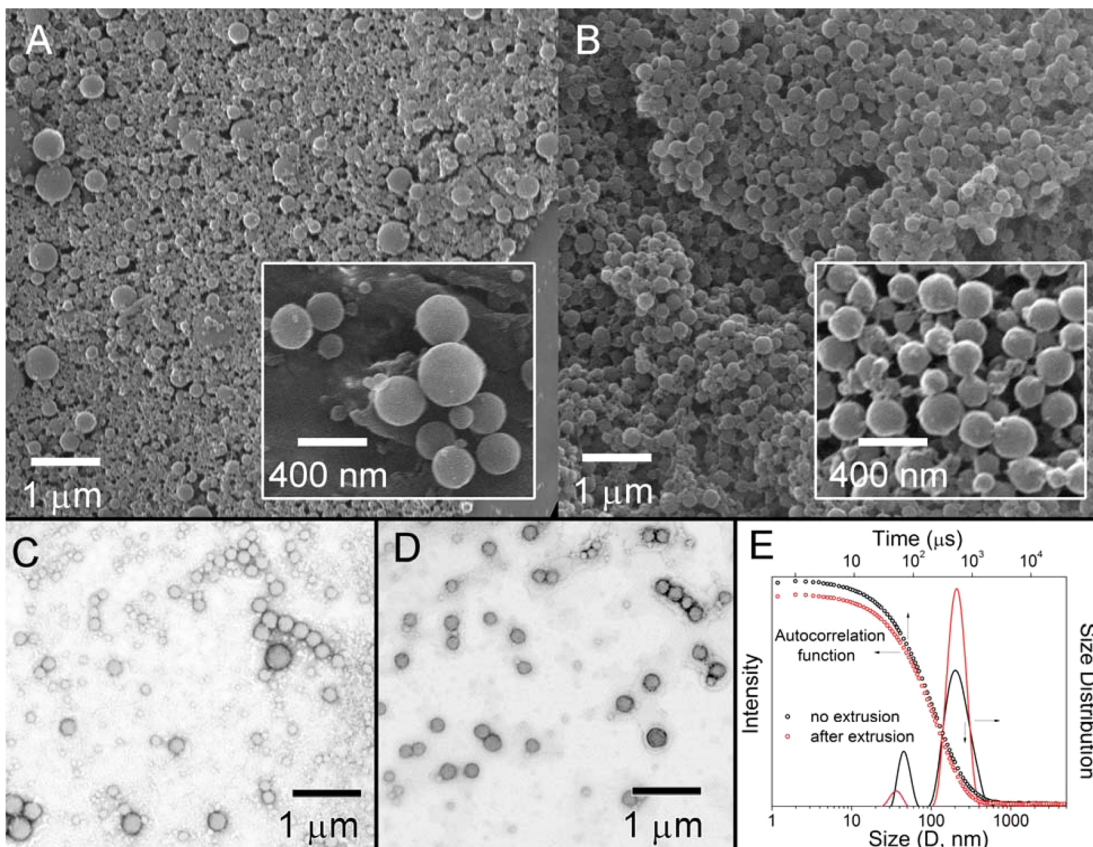


Figure 2. Morphologies of polyacrylate nanocapsules produced by the polymerization of acrylic monomers inside vesicles without (A, SEM; C, TEM) and with (B, SEM; D, TEM) an extrusion step. (E) Size distribution (solid lines) and autocorrelation function (open circles) of vesicles with acrylic monomers as determined by DLS in an aqueous solution.

acrylic monomers compared to styrene monomers.²⁶ These observations show a slightly different behavior of catanionic surfactant and lipid vesicles loaded with styrene derivatives. Our previous studies of liposomes loaded with styrene monomers showed no noticeable aggregation, suggesting the formation of stable monomer-loaded liposomes.^{2,17}

At temperatures above 50 °C, we observed vesicles in the DLS data; however, monomers started to separate from the aqueous solution and form droplets at the top of the aqueous reaction mixture. Styrene monomers started to separate at lower temperature (35 °C). Decreasing the number of styrene monomers in surfactant/monomer assemblies resulted in a decreasing vesicles diameter, and for the 1:8 molar ratio of monomers to surfactants, only micelles were present in the mixture (Figure S1C). DLS of surfactants with acrylic monomers also showed the presence of a small number of small aggregates, attributed to surfactant micelles. These aggregates are likely to be micelles and wormlike micelle aggregates as suggested by small-angle neutron scattering (SANS) studies described previously.²⁷ In summary, vesicles loaded with acrylic monomers can be stable at temperatures below 50 °C.

After the spontaneous formation of monomer-loaded vesicles, one may perform extrusion so as to narrow the size distribution of vesicles, or these vesicles can be used directly without the extrusion. We used both types of vesicles, prepared with and without extrusion, in further experiments aiming at the synthesis of nanocapsules. The correlograms obtained from the DLS measurements from both types of samples were fairly

close to a typical monomodal distribution (open circles in Figure 2E), suggesting that the predominant scattering occurred from vesicles. Following time-resolved studies evaluating polymerization versus temperature, the initiator/activator ratio, and the molar ratio of monomer to initiator/activator described in detail below, we found conditions for the complete polymerization of monomers in the bilayers that produced hollow polymer nanocapsules reproducibly. Typical results are shown in Figure 2. The average sizes of nanocapsules isolated after the polymerization of monomers and measured by SEM (Figure 2A,B) were identical to the average sizes of vesicles observed by DLS (Figure 2E). The capsules preserved their spherical shape upon drying, suggesting a high degree of cross-linking, similarly to hollow nanocapsules templated by liposomes^{2,17} and surfactant vesicles^{26,27} and produced using UV-initiated polymerization. The hollow structure was confirmed by dye-retention experiments as described below. In addition, performing SEM measurements at high voltage revealed a small fraction of collapsed capsules, further confirming their hollow structure (data not shown).

Kaler et al.⁵⁰ showed that SDBS-rich vesicles without monomers were less polydisperse than CTAT-rich vesicles. Using an extrusion technique allows us to obtain polymer nanocapsules with a narrow size distribution. Compared to nonextruded vesicles (Figure 2E, black line and circles for vesicles; Figure 2A,C for polymer nanocapsules), using extrusion before polymerization leads to the formation of uniform, spherical nanocapsules (Figure 2B,D; average diameter from SEM data approx. 220 ± 10 nm).

Combined SEM, TEM, and DLS data suggest that extrusion decreases the number of vesicles of larger diameter in the overall sample. The predominant population of nanocapsules produced with or without extrusion falls within a reasonably narrow size range and matches the size of spontaneously formed catanionic vesicles. For practical purposes, the choice of whether to perform extrusion should be made on the basis of the need for more uniform nanocapsules versus the ease of manufacturing.

To determine the optimal conditions for polymerization, we conducted a series of experiments where the conversion of monomers was measured as a function of temperature, initiator/activator molar ratio, and molar percentage of the initiator/activator pair relative to the total number of monomers and cross-linkers in the bilayer (Figure 3).

Our goal was to accomplish polymerization within a reasonable amount of time in the target temperature range of 35–40 °C. We found that polymerization can be accomplished within 2 h at 40 °C or 3 h at 35 °C (Figure 3A). When vesicles loaded with monomers and cross-linkers and initiator/activator were monitored at 25 °C, no polymerization was observed during the first 2 h (Figure 3A). The incubation of the same vesicles at 30 °C did not result in measurable polymerization during the first hour (Figure 3A). In samples incubated at both 25 and 30 °C, polymerization occurred rapidly after the initial incubation period (Figure 3A). These data suggest that the samples can be prepared and handled at temperatures below 30 °C long enough without the risk of premature polymerization and that polymerization is activated readily in the desired temperature range of 35–40 °C.

We found that the following general approach is especially convenient. Two aqueous stock solutions are prepared separately, one containing SDBS with monomers, cross-linkers, and an initiator and the other containing CTAT with monomers, cross-linkers, and an activator. These stock solutions can be handled and stored under ambient conditions for at least several days without any evidence of premature polymerization. In this study, we used freshly prepared stock solutions to ensure reproducibility. Upon combining these solutions and with a short incubation, the resulting mixture contains spontaneously formed vesicles with monomers, cross-linkers, initiator, and activator in the hydrophobic interior of the surfactant bilayer. This mixture is now ready for polymerization. The removal of oxygen and further incubation at slightly elevated temperatures for 1 to 2 h has led to the formation of hollow polymer nanocapsules.

The polymerization of a single chain in an individual vesicle is expected to be fast because of the combined effects of a highly effective monomer concentration and the alignment of monomers along templates in the hydrophobic bilayer. Full growth of individual polymer chains is attained prior to interaction with other radicals that may enter the same vesicle. Evidence for fast propagation is obtained from the kinetics of polymerization of monomers (Figures 3, S2, S3, S6, and S7). As expected, a decreasing amount of activator resulted in a substantial decrease in the initial rate of polymerization (Figure 3B). The fastest polymerization was observed for initiator to activator ratios of 1:1 and 1:2 (Figure 3B). Lowering the amount of activator further requires more than 6 h to achieve >90% conversion of monomers (Figure 3B).

Decreasing amounts of both initiator and activator at constant initiator/activator ratio of 2:1 significantly reduces monomer conversion (Figure 3C). For example, for a

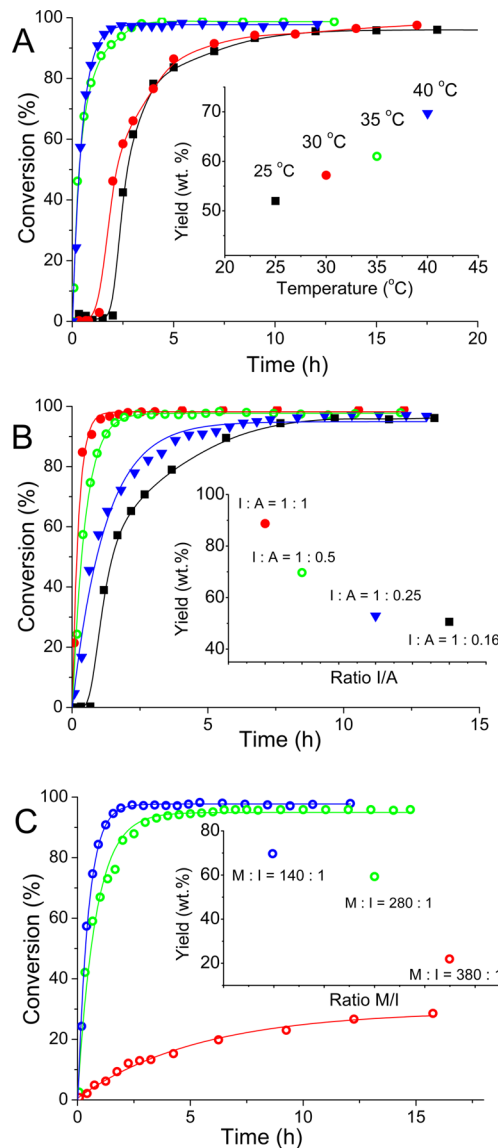


Figure 3. Typical data for conversion vs time and yield of nanocapsules. SDBS/CTAT = 80:20 wt %; 1% (w/v) solution in water of acrylic monomers/surfactants = 2:1. (A) Temperature dependence, $C_m(LP) = 4 \times 10^{-4}$ M, $C_m(MDA) = 2 \times 10^{-4}$ M, monomers/initiator = 140:1, initiator/activator = 2:1. (B) Effect of initiator to activator ratio, $T = 40$ °C, $C_m(LP) = 4 \times 10^{-4}$ M, monomers/initiator = 140:1. (C) Effect of initiator + activator concentration, $T = 40$ °C, I/A = 2:1.

monomer to initiator ratio of about 380:1 ($LP, 1.5 \times 10^{-4}$ M; $MDA, 0.75 \times 10^{-4}$ M), polymerization is clearly not practical at the desired temperature (Figure 3C). To gain further insight into the polymerization process, we addressed potential activation with the help of the surfactants that make up the bilayer. Quaternary ammonium salts, such as cetyltrimethylammonium bromide (CTAB) acting together with benzoyl peroxide, can initiate polymerization in polar solvents.⁵¹ CTAT, used here as the cationic component of the vesicle, also contains a tertiary amine moiety, but it is facing the aqueous phase and is not expected to participate significantly in the radical-formation process inside the bilayer. Furthermore, aliphatic amines are less reactive than aromatic amines used here as activators.⁵¹ We performed a series of experiments with samples containing the initiator (lauroyl peroxide) but no

activator in the bilayer. The conversion of monomers after polymerization at 40 °C for 5 h for composition SDBS/CTAT = 80:20 was very insignificant (less than 2%).

In vesicles enriched with CTAT (SDBS/CTAT = 20:80), the conversion of monomers after 5 h of polymerization was up to 15%. In all, we concluded that quarternary ammonium groups of the surfactants play only a minor role, if any, in the formation of nanocapsules. To confirm this conclusion, we performed the polymerization of acrylic monomers in the presence of both initiator and activator molecules at different compositions of the surfactant bilayer. We found no effect of the SDBS/CTAT ratio on the yield of nanocapsules (Figure S2B). These observations suggest that the polymerization process occurs primarily in the tail of the surfactants or the hydrophobic region of vesicles.

We conducted a series of experiments with styrene monomers to evaluate their polymerization within the bilayer. As expected, the reactivity of styrene monomers is substantially lower than the reactivity of acrylic monomers.⁵¹ The detailed kinetics of styrene polymerization is shown in the Supporting Information (Figures S2 and S3). The behavior of styrene monomers paralleled that of acrylic monomers, e.g., lower initiator/activator amounts resulted in slower polymerization and a smaller monomer/surfactant ratio resulted in faster polymerization with higher yields. Considering general trends in the rates of polymerization and the yield of polymer material, we conclude that optimal conditions can be found by varying the temperature, reaction time, ratio of initiator to activator, and ratio of initiator/activator to monomer/cross-linkers. We also examined the polymerization of cross-linkers alone without monomers. The initial kinetics of EDGMA polymerization is similar to polymerization of the acrylic monomer mixture, but after about 65% conversion is reached (after 3 h), the rate of polymerization significantly slows (Figure S6) as a result of increasing viscosity resulting from cross-linking. However, DVB used as a cross-linking agent for styrene-based monomers is more reactive and showed faster conversion (Figure S7).

Attempts to polymerize BMA without a cross-linking agent resulted in the formation of a linear polymer stabilized in solution by surfactants. As expected, no freestanding capsules were formed; the reaction mixture turned clear upon addition of methanol that dissolved surfactants. DLS showed no particles with a size comparable to that of the original vesicles.

We used permeability assays to evaluate the quality of nanocapsules formed by the new thermal initiation method. In these experiments, we created nanocapsules in the presence of molecules with different cross sections acting as size probes.

After the polymerization and removal of the surfactant scaffold, we washed nanocapsules to remove any molecules that escape from the capsule interior. Molecules smaller than the pore size escape from the capsules, and molecules larger than the pore size remain entrapped. Capsules with pinhole defects larger than the size probes would not be able to retain encapsulated molecules. We prepared nanocapsules with three different encapsulated colored size-probe dyes whose chemical structures are shown in Figure 4B. To do that, monomer-loaded surfactant vesicles were formed in aqueous solutions of respective dyes. The dye molecules were located both inside and outside the surfactant vesicles. After the synthesis, nanocapsules were washed thoroughly with methanol and water to remove nonentrapped dyes. Washing steps were repeated multiple times until the supernatant became colorless. Nanocapsules with Procion turquoise MX-G (PT, 1.3 nm

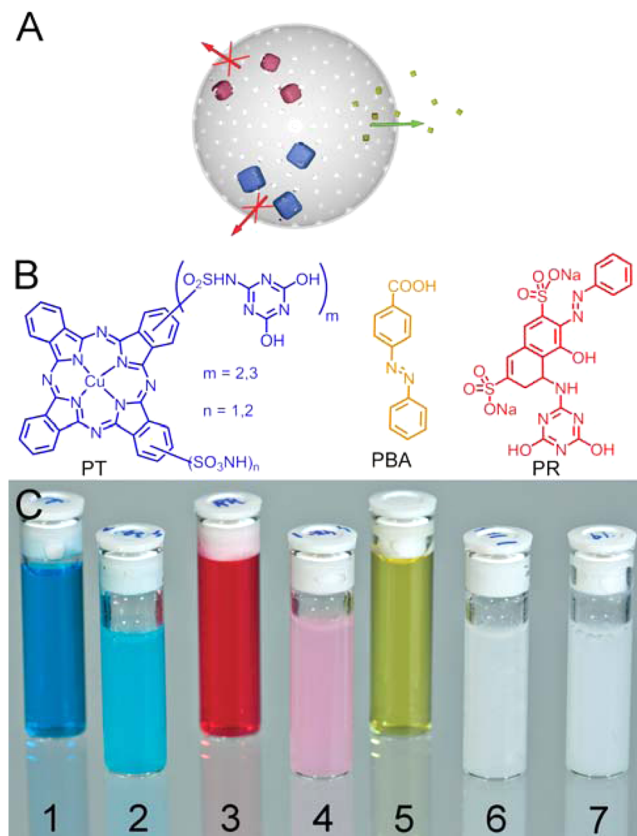


Figure 4. (A) Schematic representation of transport across the capsule wall of molecules smaller than pores and retention of larger entrapped probes. (B) Chemical structures of encapsulated dyes. (C) Photograph of the nanocapsule suspensions (2, 4, 6, 7) and solutions of free dyes (1, 3, 5): (1) solution of PT; (2) suspension of nanocapsules, prepared in the presence of PT, after surfactant removal, extensive washing in methanol, and resuspension in water, demonstrating the retention of the 1.3 nm probe; (3) solution of PR; (4) suspension of nanocapsules, prepared in the presence of PR, after surfactant removal, extensive washing in methanol, and resuspension in water, demonstrating the retention of the 1.1 nm probe; (5) solution of PBA; (6) suspension of nanocapsules, prepared in the presence of PBA, after surfactant removal, extensive washing in methanol, and resuspension in water, demonstrating complete release of the 0.6 nm probes; and (7) suspension of blank nanocapsules.

smallest cross section) and Procion red (PR, 1.1 nm smallest cross section) remained colored after complete separation from the nonentrapped dyes. At the same time, nanocapsules with 4-(phenylazo)benzoic acid (PBA, 0.6 nm smallest cross section) were bright yellow after synthesis but turned colorless after the second wash. We conclude that the walls of the capsules were permeable to smaller PBA molecules and impermeable to larger PT and PR molecules (Figure 4A).

4. CONCLUSIONS

This work addressed the challenge of creating a nanometer-thick shell with no pinhole defects using bilayer-templated directed assembly under near-physiological conditions. Controlled polymerization within the hydrophobic interior of vesicles by this technique is convenient and versatile and offers the potential to control all aspects of the nanocapsule architecture and properties through the appropriate choice of surfactants, monomers, comonomers, and polymerization conditions. Efficient cross-linking thermopolymerization, with-

out any exposure to UV light, makes the system technologically attractive for encapsulating fragile molecules such as enzymes, catalysts, and light-sensitive compounds and creating semi-permeable polymer capsule shells without damaging entrapped molecules. In addition, the synthetic compositions (i.e., highly dilute surfactant solution and a small number of monomers) and mild conditions (i.e., the temperature can be tuned in the region of 25–40 °C and the pH can be tuned in the region of 5.0–8.0) are close to the physiological conditions, further facilitating the use of polymer nanocapsules in biomedical applications. These findings enhance the directed assembly technology for the synthesis of nanocapsules and set the stage for practical applications such as nanoreactors and optical sensors.

■ ASSOCIATED CONTENT

Supporting Information

Additional experimental data. NMR and UV-vis spectra. This material is available free of charge via the Internet at <http://pubs.acs.org>

■ AUTHOR INFORMATION

Corresponding Author

*E-mail: eugene.pinkhassik@uconn.edu.

Author Contributions

The manuscript was written through the contributions of all authors. All authors have given approval to the final version of the manuscript.

Notes

The authors declare no competing financial interest.

■ ACKNOWLEDGMENTS

This work was supported by the National Science Foundation (CHE-1012951, CHE-1316680, and CHE-1522525).

■ REFERENCES

- (1) Becerra, F.; Soltero, J. F. A.; Puig, J. E.; Schulz, P. C.; Esquena, J.; Solans, C. Free-radical polymerization of styrene in worm-like micelles. *Colloid Polym. Sci.* **2003**, *282*, 103–109.
- (2) Dergunov, S. A.; Kesterson, K.; Li, W.; Wang, Z.; Pinkhassik, E. Synthesis, Characterization, and Long-Term Stability of Hollow Polymer Nanocapsules with Nanometer-Thin Walls. *Macromolecules* **2010**, *43*, 7785–7792.
- (3) Dergunov, S. A.; Miksa, B.; Ganus, B.; Lindner, E.; Pinkhassik, E. Nanocapsules with “invisible” walls. *Chem. Commun.* **2010**, *46*, 1485–1487.
- (4) Gomes, J. F. P. d. S.; Sonnen, A. F. P.; Kronenberger, A.; Fritz, J.; Coelho, M. Á. N.; Fournier, D.; Fournier-Nöel, C.; Mauzac, M.; Winterhalter, M. Stable Polymethacrylate Nanocapsules from Ultraviolet Light-Induced Template Radical Polymerization of Unilamellar Liposomes. *Langmuir* **2006**, *22*, 7755–7759.
- (5) Jintoku, H.; Okazaki, Y.; Ono, S.; Takafuji, M.; Ihara, H. Incorporation and Template Polymerization of Styrene in Single-walled Bilayer Membrane Nanotubes. *Chem. Lett.* **2011**, *40*, 561–563.
- (6) Ki, C. D.; Chang, J. Y. Preparation of a Molecularly Imprinted Polymeric Nanocapsule with Potential Use in Delivery Applications. *Macromolecules* **2006**, *39*, 3415–3419.
- (7) Lai, W. C.; Tseng, S. C.; Tung, S. H.; Huang, Y. E.; Raghavan, S. R. Nanostructured polymers prepared using a self-assembled nano-fibrillar scaffold as a reverse template. *J. Phys. Chem. B* **2009**, *113*, 8026–8030.
- (8) Ruysschaert, T.; Germain, M.; Gomes, J. F.; Fournier, D.; Sukhorukov, G. B.; Meier, W.; Winterhalter, M. Liposome-based nanocapsules. *IEEE Trans. Nanobiosci.* **2004**, *3*, 49–55.
- (9) Tekobo, S.; Pinkhassik, E. Directed covalent assembly of rigid organic nanodisks using self-assembled temporary scaffolds. *Chem. Commun.* **2009**, *9*, 1112–1114.
- (10) Tekobo, S.; Richter, A.; Dergunov, S. A.; Pingali, S.; Urban, V.; Yan, B.; Pinkhassik, E. Synthesis, characterization, and controlled aggregation of biotemplated polystyrene nanodisks. *J. Nanopart. Res.* **2011**, *13*, 6427–6437.
- (11) Mehler, E. L.; Fuxreiter, M.; Simon, I.; Garcia-Moreno, E. B. The role of hydrophobic microenvironments in modulating pKa shifts in proteins. *Proteins* **2002**, *48*, 283–292.
- (12) Isom, D. G.; Castaneda, C. A.; Cannon, B. R.; Garcia-Moreno, B. Large shifts in pKa values of lysine residues buried inside a protein. *Proc. Natl. Acad. Sci. U.S.A.* **2011**, *108*, 5260–5265.
- (13) Chen, Q.; Schönher, H.; Vancso, G. J. Block-Copolymer Vesicles as Nanoreactors for Enzymatic Reactions. *Small* **2009**, *5*, 1436–1445.
- (14) Meier, W. Polymer nanocapsules. *Chem. Soc. Rev.* **2000**, *29*, 295–303.
- (15) McKelvey, C. A.; Kaler, E. W. Characterization of nanostructured hollow polymer spheres with small-angle neutron scattering (SANS). *J. Colloid Interface Sci.* **2002**, *245*, 68–74.
- (16) McKelvey, C. A.; Kaler, E. W.; Zasadzinski, J. A.; Coldren, B.; Jung, H. T. Templating hollow polymeric spheres from catanionic equilibrium vesicles: synthesis and characterization. *Langmuir* **2000**, *16*, 8285–8290.
- (17) Dergunov, S. A.; Pinkhassik, E. Functionalization of Imprinted Nanopores in Nanometer-Thin Organic Materials. *Angew. Chem., Int. Ed.* **2008**, *47*, 8264–8267.
- (18) Dergunov, S. A.; Durbin, J.; Pattanaik, S.; Pinkhassik, E. pH-mediated catch and release of charged molecules with porous hollow nanocapsules. *J. Am. Chem. Soc.* **2014**, *136*, 2212–5.
- (19) Morgan, J. D.; Johnson, C. A.; Kaler, E. W. Polymerization of Equilibrium Vesicles. *Langmuir* **1997**, *13*, 6447–6451.
- (20) Hotz, J.; Meier, W. Vesicle-Templated Polymer Hollow Spheres. *Langmuir* **1998**, *14*, 1031–1036.
- (21) Langowska, K.; Palivan, C. G.; Meier, W. Polymer nanoreactors shown to produce and release antibiotics locally. *Chem. Commun.* **2013**, *49*, 128–130.
- (22) Sauer, M.; Streich, D.; Meier, W. pH-Sensitive Nanocontainers. *Adv. Mater.* **2001**, *13*, 1649–1651.
- (23) Aguirre, G.; Ramos, J.; Heuts, J. P. A.; Forcada, J. Biocompatible and thermo-responsive nanocapsule synthesis through vesicle templating. *Polym. Chem.* **2014**, *5*, 4569–4579.
- (24) Banner, L. T.; Danila, D. C.; Sharpe, K.; Durkin, M.; Clayton, B.; Anderson, B.; Richter, A.; Pinkhassik, E. Controlled Loading of Building Blocks into Temporary Self-Assembled Scaffolds for Directed Assembly of Organic Nanostructures. *Langmuir* **2008**, *24*, 11464–11473.
- (25) Dergunov, S. A.; Schaub, S. C.; Richter, A.; Pinkhassik, E. Time-Resolved Loading of Monomers into Bilayers with Different Curvature. *Langmuir* **2009**, *26*, 6276–6280.
- (26) Kim, M. D.; Dergunov, S. A.; Richter, A. G.; Durbin, J.; Shmakov, S. N.; Jia, Y.; Kenbeilova, S.; Orazbekuly, Y.; Kengpeil, A.; Lindner, E.; Pingali, S. V.; Urban, V. S.; Weigand, S.; Pinkhassik, E. Facile Directed Assembly of Hollow Polymer Nanocapsules within Spontaneously Formed Catanionic Surfactant Vesicles. *Langmuir* **2014**, *30*, 7061–7069.
- (27) Dergunov, S. A.; Richter, A. G.; Kim, M. D.; Pingali, S. V.; Urban, V. S.; Pinkhassik, E. Synergistic self-assembly of scaffolds and building blocks for directed synthesis of organic nanomaterials. *Chem. Commun.* **2013**, *49*, 11026–11028.
- (28) Kim, M. D.; Dergunov, S. A.; Lindner, E.; Pinkhassik, E. Dye-Loaded Porous Nanocapsules Immobilized in a Permeable Polyvinyl Alcohol Matrix: A Versatile Optical Sensor Platform. *Anal. Chem.* **2012**, *84*, 2695–2701.
- (29) Peters, R. J. R. W.; Marguet, M.; Marais, S.; Fraaije, M. W.; van Hest, J. C. M.; Lecommandoux, S. Cascade Reactions in Multi-compartmentalized Polymericosomes. *Angew. Chem., Int. Ed.* **2014**, *53*, 146–150.

- (30) Meeuwissen, S. A.; Rioz-Martinez, A.; de Gonzalo, G.; Fraaije, M. W.; Gotor, V.; van Hest, J. C. M. Cofactor regeneration in polymersome nanoreactors: enzymatically catalysed Baeyer-Villiger reactions. *J. Mater. Chem.* **2011**, *21*, 18923–18926.
- (31) Vriezema, D. M.; Garcia, P. M. L.; Sancho Oltra, N.; Hatzakis, N. S.; Kuiper, S. M.; Nolte, R. J. M.; Rowan, A. E.; van Hest, J. C. M. Positional Assembly of Enzymes in Polymersome Nanoreactors for Cascade Reactions. *Angew. Chem., Int. Ed.* **2007**, *46*, 7378–7382.
- (32) Vriezema, D. M.; Comellas Aragones, M.; Elemans, J. A. A. W.; Cornelissen, J. J. L. M.; Rowan, A. E.; Nolte, R. J. M. Self-Assembled Nanoreactors. *Chem. Rev.* **2005**, *105*, 1445–1490.
- (33) Kim, K. T.; Cornelissen, J. J. L. M.; Nolte, R. J. M.; van Hest, J. C. M. A Polymersome Nanoreactor with Controllable Permeability Induced by Stimuli-Responsive Block Copolymers. *Adv. Mater.* **2009**, *21*, 2787–2791.
- (34) Rikken, R. S. M.; Kerkenaar, H. H. M.; Nolte, R. J. M.; Maan, J. C.; van Hest, J. C. M.; Christianen, P. C. M.; Wilson, D. A. Probing morphological changes in polymersomes with magnetic birefringence. *Chem. Commun.* **2014**, *50*, 5394–5396.
- (35) Chen, T.; Du, B.; Fan, Z. Facile Fabrication of Polymer Nanocapsules with Cross-Linked Organic–Inorganic Hybrid Walls. *Langmuir* **2012**, *28*, 11225–11231.
- (36) Chen, T.; Du, B.; Zhang, X.; Fan, Z. Fabrication of Polymer Nanocapsules with Controllable Oligo(Ethylene Glycol) Densities, Permeation Properties and Robustly Crosslinked Walls. *ACS Appl. Mater. Interfaces* **2013**, *5*, 3748–3756.
- (37) Yow, H. N.; Routh, A. F. Formation of liquid core-polymer shell microcapsules. *Soft Matter* **2006**, *2*, 940–949.
- (38) Yu, X.; Zhao, Z.; Nie, W.; Deng, R.; Liu, S.; Liang, R.; Zhu, J.; Ji, X. Biodegradable Polymer Microcapsules Fabrication through a Template-Free Approach. *Langmuir* **2011**, *27*, 10265–10273.
- (39) Zhang, J.; Ge, X.; Wang, M.; Yang, J.; Wu, Q.; Wu, M.; Liu, N.; Jin, Z. Hybrid hollow microspheres templated from double Pickering emulsions. *Chem. Commun.* **2010**, *46*, 4318–4320.
- (40) Dudman, W. F.; Bishop, C. T. Electrophoresis of dyed polysaccharides on cellulose acetate. *Can. J. Chem.* **1968**, *46*, 3079–3084.
- (41) Meltzer, T. H.; Tobolsky, A. V. Kinetics of polymerization of styrene initiated by the system benzoyl peroxide-dimethylaniline. *J. Am. Chem. Soc.* **1954**, *76*, 5178–5180.
- (42) Nishimura, N. Dead-end polymerization of styrene and methyl methacrylate in the benzoyl peroxide-dimethylaniline redox system. *J. Polym. Sci., Part A-1: Polym. Chem.* **1969**, *7*, 2015–2020.
- (43) O'Driscoll, K. F.; Richezza, E. N. Polymerization with oxidation-reduction initiators. III. Complex formation between benzoyl peroxide and dimethylaniline. *J. Polym. Sci.* **1960**, *46*, 211–216.
- (44) O'Driscoll, K. F.; Schmidt, J. F. Polymerization with oxidation-reduction initiators. II. The system styrene-benzoyl peroxide-dimethylaniline at elevated temperatures. *J. Polym. Sci.* **1960**, *45*, 189–194.
- (45) O'Driscoll, K. F.; White, P. J. Kinetics of polymerization of styrene initiated by substituted benzoyl peroxides. I. Effect of thermal initiation. *J. Polym. Sci., Part B1: Polym. Lett.* **1963**, *1*, 597–599.
- (46) Senel, S.; Isik-Yurukosoy, I.; Guven, O. A kinetic study of homogeneous bulk polymerization of ethyl methacrylate initiated by benzoyl peroxide and an N,N-dimethylaniline redox pair. *Turk. J. Chem.* **1996**, *20*, 62–68.
- (47) Walling, C.; Indictor, N. Solvent effects and initiator efficiency in the benzoyl peroxide-dimethylaniline system. *J. Am. Chem. Soc.* **1958**, *80*, 5814–5818.
- (48) Wilson, G. O.; Henderson, J. W.; Caruso, M. M.; Blaiszik, B. J.; McIntire, P. J.; Sottos, N. R.; White, S. R.; Moore, J. S. Evaluation of peroxide initiators for radical polymerization-based self-healing applications. *J. Polym. Sci., Part A: Polym. Chem.* **2010**, *48*, 2698–2708.
- (49) Kumar, S.; Kim, D.-W.; Lee, H.-J.; Changez, M.; Yoon, T.-H.; Lee, J.-S. Exploration of the Mechanism for Self-Emulsion Polymerization of Amphiphilic Vinylpyridine. *Macromolecules* **2013**, *46*, 7166–7172.
- (50) Kaler, E. W.; Murthy, A. K.; Rodriguez, B. E.; Zasadzinski, J. A. Spontaneous vesicle formation in aqueous mixtures of single-tailed surfactants. *Science* **1989**, *245*, 1371–1374.
- (51) Mishra, M. K., Yagci, Y., Eds.; *Handbook of Vinyl Polymers: Radical Polymerization, Process, and Technology*, 2nd ed. CRC Press/Taylor & Francis: 2009.